Desalination and Water Treatment
www.deswater.com

doi: 10.1080/19443994.2015.1101018

57 (2016) 19510–19518
September

Taylor & Francis
Taylor & Francis Group

Kinetic modeling and error analysis for zinc removal on a weak base anion exchange resin

Emilia Gîlcă, Andrada Măicăneanu*, Adina Ghirişan, Petru Ilea

Faculty of Chemistry and Chemical Engineering, Department of Chemical Engineering, Babeş-Bolyai University, 11 Arany Janos Street, 400028 Cluj Napoca, Romania, Tel. +40 264 593833, ext. 5631; Fax: +40 264 590818; email: gemilia@chem.ubbcluj.ro (E. Gîlcă), Tel. +40 264 593833, ext. 5737; Fax: +40 264 590818; email: andrada@chem.ubbcluj.ro (A. Măicăneanu), Tel. +40 264 593833, ext. 5663; Fax: +40 264 590818; email: ghirisan@chem.ubbcluj.ro (A. Ghirişan), Tel. +40 264 593833, ext. 5678; Fax: +40 264 590818; email: pilea@chem.ubbcluj.ro (P. Ilea)

Received 7 January 2015; Accepted 22 September 2015

ABSTRACT

The efficiency of Purolite A103S resin for zinc removal (as zinc chloride complexes) has been studied using different resin quantities and temperatures in a batch adsorption system. The experimental data were analyzed using pseudo-first-order, pseudo-second-order forms, Elovich, and intra-particle diffusion models. Kinetic studies showed that the adsorption followed type 1 pseudo-second-order reaction model. The results obtained from the kinetics models were examined by the most common error functions (e.g. ERRSQ/SSE, HYBRID, ARE, EABS, MPSD,r_s, s_{RE}, S.E., RMSE, APE, and Δq). Thermodynamic parameters, enthalpy, entropy, and Gibbs free energy were calculated in order to determine the adsorption behavior. The enthalpy value indicated an exothermic reaction. The activation energy value suggested that the process that rules over the zinc sorption on the Purolite A103S resin is physical.

Keywords: Zinc chloride; Kinetics; Error functions; Thermodynamics

1. Introduction

One of the oldest technique used to protect iron or steel pieces from corrosion processes is hot-dip galvanizing, which is based on dipping the pieces into molten zinc. The effluents coming from the pickling process, used to prepare steel pieces for galvanizing, contain high concentrations of Zn, Fe, and HCl together with low concentrations of organic compounds, such as hydrogen evolution reaction inhibitors, and other heavy metals. Therefore, spent pickling baths have to be treated before their disposal to accomplish with the environmental restrictions [1]. Until now different combination of technologies such as ion exchange, liquid–liquid extraction and pyrohydrolysis, solvent extraction and evaporation, anion exchange and oxidation, anion exchange and acid retardation, anion exchange and membrane electrowinning have been studied [2].

The most popular removal materials are ion exchangers/zeolites whereby zinc can exchange preferentially with other ions [3]. The main advantages of ion exchange are the recovery of metal, selectivity, less sludge produced, high adsorption capacity, and can reduce the metal ion concentration to a very low level [4].

A number of investigators have studied the removal of zinc ions from aqueous waste solution using natural, synthetic, chelating ion exchange resins,

*Corresponding author.

and it was found that this method can be suitable for industrial wastewater treatment [5,6].

In hydrochloric acid effluents, the main species present as anionic species are zinc chloride complexes [2]. Marañón et al. proposed two alternatives for the treatment of acid pickling baths using anion-exchange resins: one-step removal (treatment in a single exchange column with prior oxidation of Fe^{2+}–Fe^{3+}) or two-step removal (two exchange columns in series, removing Zn in the first, and Fe in the second after oxidation to Fe^{3+}) [7]. The aim of the present work was to examine the performance of Purolite A103S, an anion-exchange resin to remove zinc as zinc chloride complexes in a batch adsorption system taken into consideration the influence of resin quantity and temperature, and the error analysis of the obtained results.

2. Materials and methods

2.1. Resins and solutions

Before usage, Purolite A103S a macroporous polystyrenic weak base anion resin was soaked in double-distilled water for 24 h. The stock solution (500 mg/L) was prepared by dissolving $ZnCl_2$ salt in 3 M HCl in order to ensure the formation of zinc complexes. All chemicals used were of analytical grade.

2.2. Apparatus and analytical procedure

Batch sorption experiments were performed on a magnetic stirrer at 300 rpm using beakers containing 100 mL zinc solution with 500 mg/L initial concentration, contacted for 300 min. In order to determine the sorption conditions, experiments were conducted with different resin quantities (1–5 g) and temperatures (297, 314, 329, 344, and 359 K). At predetermined time intervals, samples from beakers were taken and analyzed using an atomic absorption spectrophotometer Avanta PM GBC (Australia). All experiments were performed in triplicate and the average value was taken for further calculations.

The ionic exchange capacity, q_e (mg/g), was calculated using Eq. (1), while removal efficiency, $E(\%)$ was calculated using Eq. (2):

$$q_e = \frac{(C_o - C_e)}{m} \times \frac{V}{1000} \quad (1)$$

$$E(\%) = \frac{C_o - C_e}{C_o} \times 100 \quad (2)$$

where C_o and C_e are the initial and equilibrium zinc ion concentrations (mg/L), respectively, V is the volume of the zinc solution (mL), and m is the mass of the resin (g) [6].

3. Results and discussion

3.1. Effect of resin quantity and contact time

Sorption experiments were carried out at various resin quantities (1–5 g) and fixed initial zinc concentration (500 mg/L). The results are given in Fig. 1. The sorption capacity increased with decreasing the resin quantity, from 10 to 46 mg/g. This could be due to partial overlapping or aggregation of adsorbent at higher resin quantities, resulting in a decrease in total surface area and the availability of sorption sites [8]. As the resin quantity increases the removal efficiency also increases from 87 to 96% (Fig. 2). Approximately 80–90% of zinc was removed within 10–50 min and the maximum adsorption was obtained after 210 min, when the equilibrium was reached. The initial rapid rate of sorption is due to the difference in zinc concentration between the solid and liquid phase in the first stages of the process. The increase in the removal efficiency along with the increase in resin quantity can be attributed to the increased number of sites and exchangeable ions available for adsorption [9].

3.2. Effect of temperature

Temperature has an important effect on the adsorption process. The experiments were carried out using a fixed anion exchanger quantity (5 g) and initial zinc concentration (500 mg/L) at different temperatures (297–359 K). The results are presented in Fig. 3. Upon increasing the temperature the removal efficiency slowly decreases. The decrease in percentage of adsorption with the rise in temperature may be due to

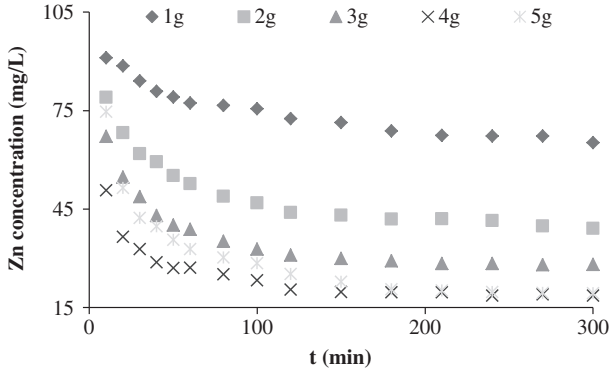

Fig. 1. Effect of resin quantity on zinc sorption by Purolite A103S; C_o = 500 mg/L, 297 K, 300 rpm.

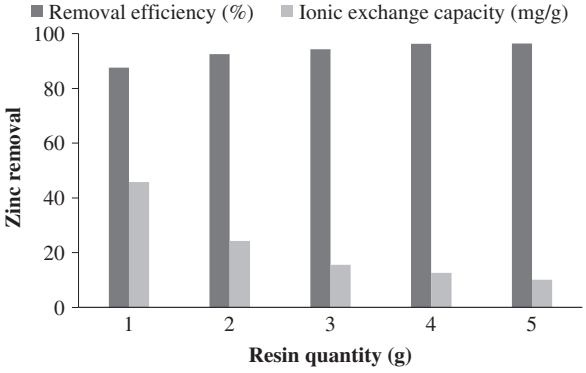

Fig. 2. Removal efficiency and ionic exchange capacity for zinc sorption on different resin quantities; C_o = 500 mg/L, m = 5 g, 297 K, 300 rpm.

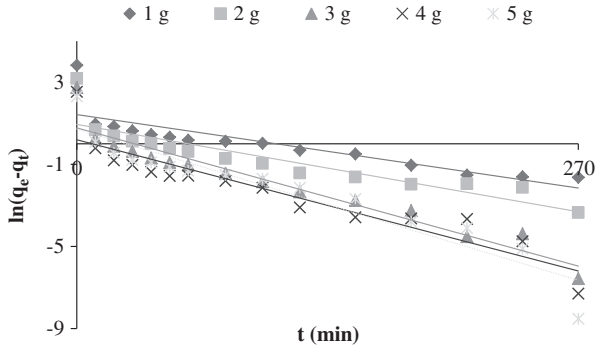

Fig. 4. Plot of pseudo-first-order reaction kinetic model for zinc sorption on Purolite A103S; C_o = 500 mg/L, 297 K, 300 rpm.

desorption caused by an increase in the available thermal energy. Higher temperature induces higher mobility of the adsorbate causing desorption [10].

3.3. Kinetic models

Prediction of batch kinetics is important for designing the sorption systems to test the experimental data, to find the mechanism of adsorption, and its rate-controlling step. Several kinetic models such as pseudo-first-order [11], pseudo-second-order [12,13], Elovich [14], and intra-particle kinetic models [15] can be applied to explain the mechanism of the adsorption processes.

Fig. 4 shows the plot for pseudo-first-order kinetic model using different resin quantities of Purolite A103S resin for zinc removal. The rate constants k_1 and the ionic exchange capacities q_t at any time, t, (mg/g) were calculated from the plot presented in Table 1, [6]. It can be observed that k_1 increases with the increase in resin quantity. The correlation coefficients were ranging from 0.7247 to 0.8899 (Table 2). Based on the obtained results, the calculated q_e values according to pseudo-first-order rate expression were in disagreement with the experimental q_e values.

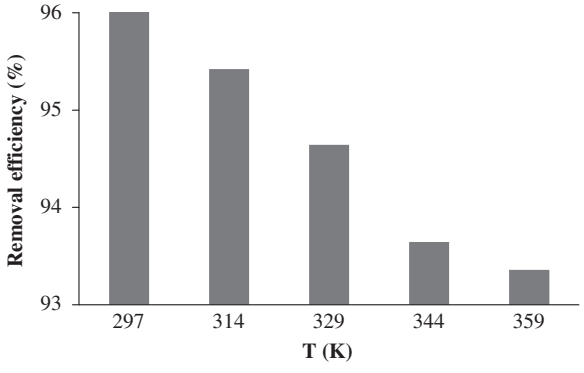

Fig. 3. Effect of temperature for zinc sorption on Purolite A103S; C_o = 500 mg/L, m = 5 g, 300 rpm.

The pseudo-second-order rate constant k_2, (g/mg min) for Type 1–4 of pseudo-second-order expressions are presented in Table 1 [16]. The calculated q_e and k_2 kinetic constants according to four linear forms of the pseudo-second-order models at different resin quantities are presented in Table 2. Moreover, Fig. 5(a)–(d) illustrates the experimental data using the equations of Types 1–4 pseudo-second-order kinetic models for zinc sorption on the considered resin. Kinetic studies for zinc sorption using different resin quantities showed a good correlation for the Type 1 pseudo-second-order expression. The high values of R^2 (Table 2) confirmed that the sorption followed a pseudo-second-order mechanism. The calculated ionic exchange capacities ($q_{e,calc}$) were in very good agreement with the experimental ionic exchange capacities. In case of Types 2–4 pseudo-second-order models, lower R^2 values (from 0.7559 to 0.9735) were obtained.

Elovich model was primarily developed to describe the kinetics of chemisorption [6,17]. The linear form of this equation is given in Table 1, where α, β known as the Elovich coefficients, represent the initial sorption rate (mg/g min) and the sorption constant [6]. The predicted kinetics constants and their corresponding R^2 values are presented in Table 2. Experimental data (Fig. 6) did not fit on the Elovich equation (small R^2 values), therefore the exchange of electrons between adsorbent and adsorbate did not take place during the sorption of zinc complexes on Purolite A103S [17]. Thus, the process that rules over the zinc sorption on the studied resin is physical. Moreover, estimated $q_{e,calc}$ values, Table 2, gave

Table 1
Kinetics models linear forms

Type	Linear form	Plot	Parameters
Pseudo-first-order	$\ln(q_e - q_t) = \ln q_e - k_1 t$	$\ln(q_e - q_t)$ vs. t	k_1 = slope q_e = intercept
Pseudo-second-order 1	$\frac{t}{q_t} = \frac{1}{k_2 q_e^2} + \frac{1}{q_e} t$	$\frac{t}{q_t}$ vs. t	q_e = 1/slope k_2 = slope^2/intercept
2	$\frac{1}{q_t} = \left(\frac{1}{k_2 q_e^2}\right)\frac{1}{t} + \frac{1}{q_e}$	$\frac{1}{q_t}$ vs. $\frac{1}{t}$	q_e = 1/intercept k_2 = intercept^2/slope
3	$q_t = q_e - \left(\frac{1}{k_2 q_e}\right)\frac{q_t}{t}$	q_t vs. $\frac{q_t}{t}$	q_e = intercept k_2 = −1/(intercept·slope)
4	$\frac{q_t}{t} = k q_e^2 - k_2 q_e q_t$	$\frac{q_t}{t}$ vs. q_t	q_e = −intercept/slope k_2 = slope^2/intercept
Elovich	$q_t = \frac{1}{\beta}\ln \alpha\beta + \frac{1}{\beta}\ln t$	q_t vs. $\ln t$	α = slope β = intercept
Intra-particle diffusion	$q_t = k_{ip} t^{0.5}$	q_t vs. $t^{0.5}$	k_{id} = slope C = intercept

Table 2
Kinetic parameters obtained for different resin quantities

Type	Parameters	1 g	2 g	3 g	4 g	5 g
Pseudo-first-order	k_1 (1/min)	0.01	0.01	0.02	0.02	0.02
	$q_{e,calc}$ (mg/g)	4.16	2.57	2.16	1.22	2.05
	R^2	0.7247	0.7953	0.9154	0.8543	0.8899
Pseudo-second-order	k_2 (g/mg min)	0.01	0.02	0.04	0.08	0.05
1	$q_{e,calc}$ (mg/g)	45.66	24.20	15.54	12.61	10.07
	R^2	1	1	1	1	1
2	k_2 (g/mg min)	0.03	0.04	0.06	0.11	0.07
	$q_{e,calc}$ (mg/g)	45.24	24.03	15.52	12.61	10.07
	R^2	0.7637	0.9009	0.9432	0.9713	0.9735
3	k_2 (g/mg min)	0.34	0.04	0.06	0.11	0.07
	$q_{e,calc}$ (mg/g)	45.33	24.07	15.49	12.61	10.07
	R^2	0.7559	0.8948	0.8911	0.9694	0.9690
4	k_2 (g/mg min)	0.02	0.03	0.05	0.10	0.07
	$q_{e,calc}$ (mg/g)	45.51	24.11	15.53	12.61	10.07
	R^2	0.7559	0.8948	0.8911	0.9690	0.9694
Elovich	α (mg/g min)	0.78	0.56	0.36	0.20	0.28
	β	41.29	21.10	13.61	11.52	8.55
	R^2	0.9881	0.9660	0.932	0.8981	0.9152
Intra-particle diffusion	k_{ip} (mg/g min$^{0.5}$)	0.38	0.71	1.11	1.37	1.71
	C	43.00	22.39	14.46	12.00	9.22
	R^2	0.9446	0.8427	0.7779	0.7363	0.7603
Experimental values	$q_{e,exp}$ (mg/g)	45.79	24.20	15.54	12.61	10.07

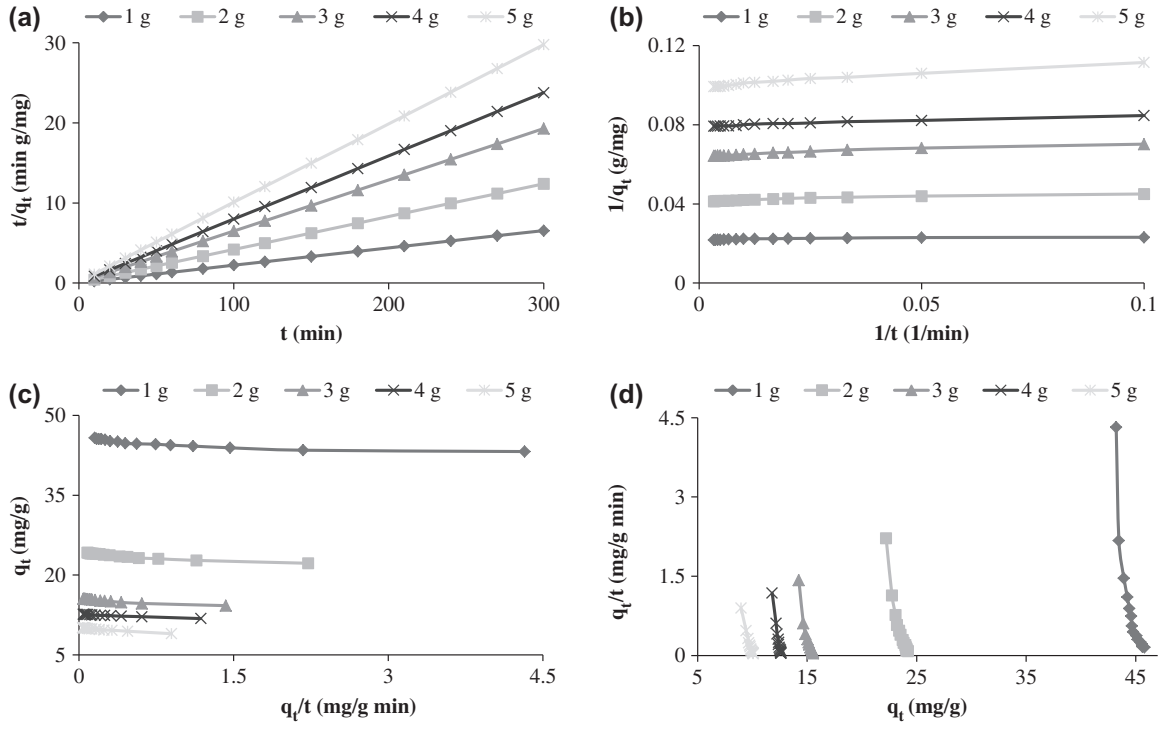

Fig. 5. Plot of pseudo-second-order types reaction kinetic model for zinc sorption on Purolite A103S; (a) Type 1, (b) Type 2, (c) Type 3, (d) Type 4; C_o = 500 mg/L, 297 K, 300 rpm.

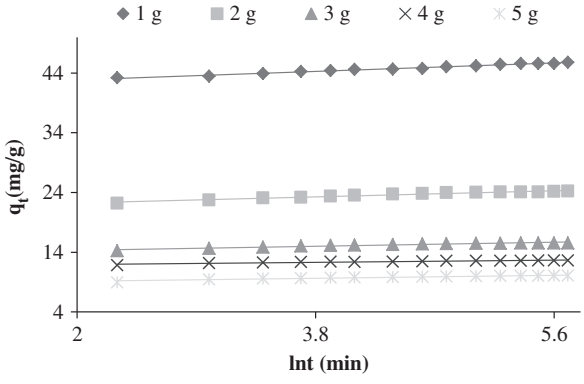

Fig. 6. Plot of Elovich kinetic model for zinc sorption on Purolite A103S; C_o = 500 mg/L, 297 K, 300 rpm.

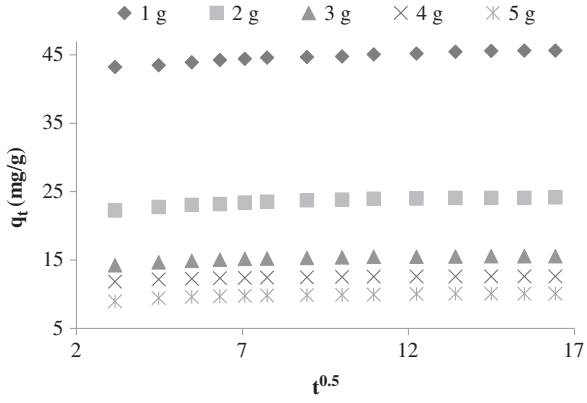

Fig. 7. Plot of intra-particle diffusion model for zinc sorption on Purolite A103S; C_o = 500 mg/L, 297 K, 300 rpm.

significantly different values compared with the experimental values.

The effects of resin quantity on the rate of sorption, when intra-particle diffusion model was applied are shown in Fig. 7. The amount of adsorbed zinc decreased approximately from 46 to 10 mg/g, when the resin quantities increased from 1 to 5 g. The calculated kinetic parameters obtained from q_t vs. $t^{0.5}$ plot are listed in Table 2. The values of intra-particle diffusion rates, k_{ip} (mg/g min$^{0.5}$) increased from 0.38 to 1.71 mg/g min$^{0.5}$ with the increase in resin quantities. This is due to the fact that the plots presented in Fig. 7 did not pass through the origin and the intercept values were higher than 0, the intra-particle diffusion was not considered to be the rate-controlling step [6,8].

It is important to note that for pseudo-first-order model, types 2–4 of pseudo-second-order, Elovich equation, and intra-particle diffusion model, the correlation coefficient was always less than 0.9881,

which indicated a bad correlation. In contrast, the application of type 1 pseudo-second-order model leads to much better regression coefficients, all around 1, leading to the conclusion that this model describes the best zinc sorption process on Purolite A103S.

3.4. Error analysis for kinetic models

Contrary to the linearization models, nonlinear regression involves the minimization or maximization of error distribution, between the experimental and the predicted data [18]. Thus, in the present study, nonlinear regression method was used to determine the optimum model out of the four widely used kinetic models studied.

Sum squares errors (ERRSQ) is the most widely used error function, at higher end of the liquid-phase concentration ranges. Hybrid fractional error function (HYBRID) was developed to improve ERRSQ fit at low concentrations. Average relative error (ARE) attempts to minimize the fractional error distribution across the entire studied concentration range. Sum of absolute errors (EABS) is similar to the ERRSQ function and provides a better fit at higher concentration. Based on to the number of degrees of freedom in the system, Marquardt's percent standard deviation (MPSD) it is similar in some respects with a modified geometric mean error distribution. Spearman's correlation coefficient (r_s) and standard deviation of relative errors (s_{RE}) are determined to evaluate the global correlation and the dispersion of their relative errors. Standard error (S.E.), root mean squared error (RMSE), average percentage errors (APE) and normalized standard deviation, Δq (%) were also considered [9,17,18]. The equations of each error function are presented in Table 3.

Table 3
List of error function applied for zinc sorption on Purolite A103S

Error function	Abbreviation	Expression
Sum squares errors	ERRSQ/SSE	$\sum_{i=1}^{n}(q_{e,calc}-q_{e,exp})^2$
Hybrid fractional error function	HYBRID	$\frac{100}{n-p}\sum_{i=1}^{n}\left[\frac{q_{e,exp}-q_{e,calc}}{q_{e,exp}}\right]_i$
Average relative error	ARE	$\frac{100}{n}\sum_{i=1}^{n}\left[\frac{q_{e,exp}-q_{e,calc}}{q_{e,exp}}\right]_i$
Sum of absolute error	EABS	$\sum_{i=1}^{n}\left\|q_{e,exp}-q_{e,calc}\right\|$
Marquardt's percent standard deviation	MPSD	$100\sqrt{\frac{1}{n-p}\sum_{i=1}^{n}\left(\frac{q_{e,exp}-q_{e,calc}}{q_{e,exp}}\right)^2}_i$
Spearman's correlation coefficient	r_s	$1-\frac{6\sum_{i=1}^{n}(q_{e,exp}-q_{e,calc})_i^2}{n(n-1)^2}$
Standard deviation of relative errors	s_{RE}	$\sqrt{\frac{\sum_{i=1}^{n}[(q_{e,exp}-q_{e,calc})_i-ARE]_i^2}{n-1}}$
Standard error	S.E.	$\sqrt{\frac{1}{n-p}\sum_{i=1}^{n}(q_{e,exp}-q_{e,calc})^2}$
Root mean squared error	RMSE	$\sqrt{\frac{1}{n}\sum_{i=1}^{n}(q_{e,calc}-q_{e,exp})^2}$
Average percentage errors	APE	$\frac{\sum_{i=1}^{n}\left\|\frac{(q_{e,exp}-q_{e,calc})}{q_{e,exp}}\right\|}{n}\times 100$
Normalized standard deviation	Δq (%)	$100\cdot\sqrt{\frac{\sum[(q_{e,exp}-q_{e,cal})/q_{e,exp}]^2}{n-1}}$

Table 4
Results obtained from different error function for the considered kinetic models

Type	Pseudo-first-order	Pseudo-second-order				Elovich	Intra-particle diffusion
		1	2	3	4		
HYBRID	656	0.009	0.05	0.04	0.01	10.84	4.53
ARE	3,923	0.96	1.04	1.03	1.01	3.05	2.11
EABS	96	0.32	0.74	0.65	0.38	12.17	7.83
MPSD	256	0.99	2.44	2.06	1.27	32.92	21.29
r_s	0.12	0.99	0.99	0.99	0.99	0.98	0.99
s_{RE}	1,037	0.27	0.13	0.15	0.19	1.16	0.72
S.E.	14.07	0.04	0.15	0.13	0.08	1.69	1.06
RMSE	13.09	0.03	0.14	0.12	0.07	1.57	0.99
APE (%)	29.07	0.12	0.13	0.12	0.06	3.93	2.62
ERRSQ/SSE	2,574	0.02	0.33	0.23	0.09	37.24	14.70
Δq (%)	52	0.12	0.37	0.31	0.19	7.17	4.82

The terms of the error functions are defined as: $q_{e,calc}$ is the theoretical ionic exchange capacity calculated from the kinetic model, $q_{e,exp}$ is the experimental ionic exchange capacity obtained from Eq. (1), n is the number of data points, and p is the number of isotherm parameters [9,17,18].

The experimental data and the calculated values obtained by applying different kinetic models were analyzed by the most common error function described above in order to compare the applicability of each model. The results are presented in Table 4.

The outcomes indicated that the pseudo-second-order kinetic model fitted the experimental data (low values for the error function). The statistical tests were able to point the pseudo-second-order model as the most appropriate one to fit the experimental data and the Elovich model as the lowest model to predict the fitting. It was found that the sorption of zinc complexes follows the Type 4 pseudo-second-order model (values of Δq are less than 5%). On the other hand, it was concluded that pseudo-first-order, Elovich, and intra-particle diffusion models overestimates zinc sorption (values of Δq are 52, 7.17, and 4.8, respectively).

3.5. Thermodynamic parameters

Thermodynamic parameters, enthalpy (ΔH°, kJ/mol), entropy (ΔS°, kJ/K mol), and Gibbs free energy (ΔG°, kJ/mol) can be used to deduce the nature of adsorption [8].

Thermodynamic parameters can be determined using the equilibrium constant, K_d (q_e/C_e), which depends on temperature. These parameters were calculated using the following equations:

$$\Delta G^\circ = -RT \ln K_d \tag{3}$$

$$\ln K_d = -\frac{\Delta H^\circ}{RT} + \frac{\Delta S^\circ}{R} \tag{4}$$

$$\Delta G^\circ = \Delta H^\circ - T\Delta S^\circ \tag{5}$$

where R is the universal gas constant (8.314×10^{-3} kJ/K mol), T is temperature (K), and K_d is the distribution coefficient (L/g).

Plot of $\ln K_d$ vs. $1/T$ is used to find the values of ΔH° and ΔS° from the slope and the intercept. The values of thermodynamic parameters are given in Table 5. The negative value for ΔH° in case of zinc sorption on Purolite A103S, suggested an exothermic interaction at temperatures between 298 and 358 K. The slight negative ΔS° value indicates that randomness decreases at the solid-solution interface during sorption. The small positive ΔG° values show the existence of an energy barrier and that the reaction is a non-spontaneous process at all studied temperatures [6,8,17].

Table 5
Thermodynamic parameters for zinc sorption on Purolite A103S

		ΔG° (kJ/mol)				
ΔS° (kJ/K mol)	ΔH° (kJ/mol)	298 K	313 K	328 K	343 K	358 K
−0.030	−9.36	1.68	2.24	2.80	3.35	3.91

3.6. Activation energy

Arrhenius equation is fitted to be used with pseudo-second-order rate constant to determine activation energy (E_a) using the following equation [8]:

$$\ln K = \ln A - \frac{E_a}{RT} \quad (6)$$

where k is the rate constant for pollutant removal (pseudo-second-order) (g/min), A is Arrhenius constant (g/min), R is the universal gas constant (8.314×10^{-3} kJ/K mol), and T is temperature (K).

Activation energy (E_a) can be calculated from linear plots $\ln k$ vs. $1/T$. The E_a value gives information about the type of sorption, either physical or chemical: physisorption process normally has activation energy of 5–40 kJ/mol, while chemisorption has higher activation energy (40–800 kJ/mol) [8]. In the case of zinc sorption on Purolite A103S, the calculated value for E_a was 32.57 kJ/mol, which indicates a physisorption process.

4. Conclusions

The zinc sorption process on the Purolite A103S resin has shown an increase in removal efficiency with an increase in resin quantity, and a slowly decrease with the increase in temperature.

By comparing the results of the values of the error functions, it was found that Type 4 pseudo-second-order model was the most suitable model to reasonably describe the studied sorption phenomenon, while Elovich model is the most inappropriate model to predict the fitting.

The thermodynamic parameters indicated an exothermic interaction, a decreased randomness at the solid-solution interface during sorption and a non-spontaneous process at the investigated temperatures. Also, the activation energy values suggested that the process which rules over the zinc sorption on Purolite A103S resin is physical.

List of symbols

q_e — ionic exchange capacity (mg/g)
E — removal efficiency (%)
C_o — initial zinc ion concentrations (mg/L)
C_e — equilibrium zinc ion concentrations (mg/L)
V — volume of zinc solution (mL)
m — mass of resin (g)
k_1 — Pseudo-first-order rate constant (1/min)
q_t — ionic exchange capacity at any time (mg/g)
$q_{e,calc}$ — calculated ionic exchange capacity (mg/g)
$q_{e,exp}$ — experimental ionic exchange capacity (mg/g)
k_2 — pseudo-second-order rate constant (g/mg min)
R^2 — correlation coefficient
α — Elovich initial sorption rate (mg/g min)
β — Elovich sorption constant
k_{ip} — intra-particle diffusion rates (mg/g $\text{min}^{0.5}$)
n — number of data points
p — number of isotherm parameters
ΔH° — enthalpy (kJ/mol)
ΔS° — entropy (kJ/K mol)
ΔG° — Gibbs free energy (kJ/mol)
R — universal gas constant (8.314×10^{-3} kJ/K mol)
T — temperature (K)
K_d — distribution coefficient (L/g)
E_a — activation energy
A — Arrhenius constant (g/min)

Acknowledgments

This paper is a result of a doctoral research made possible with the financial support of the Sectoral Operational Programme for Human Resources Development 2007–2013, co-financed by the European Social Fund, under the project POSDRU/159/1.5/S/132400-"Young successful researchers - professional development in an international and interdisciplinary environment".

References

[1] J. Carrillo-Abad, M. García-Gabaldón, V. Pérez-Herranz, Study of the zinc recovery from spent pickling baths by means of an electrochemical membrane reactor using a cation-exchange membrane under galvanostatic control, Sep. Purif. Technol. 132 (2014) 479–486.
[2] M.F. San Román, I. Ortiz Gándara, R. Ibañez, I. Ortiz, Hybrid membrane process for the recovery of major components (zinc, iron and HCl) from spent pickling effluents, J. Membr. Sci. 415–416 (2012) 616–623.
[3] T.-H. Shek, A. Ma, V.K.C. Lee, G. Mckay, Kinetics of zinc ions removal from effluents using ion exchange resin, Chem. Eng. J. 146 (2009) 63–70.
[4] G. Müller, K. Janošková, T. Bakalár, J. Cakl, H. Jiránková, Removal of Zn(II) from aqueous solutions using Lewatit S1468, Desalin. Water Treat. 37 (2012) 146–151.
[5] O. Abdelwahab, N.K. Amin, E.-S.Z. El-Ashtoukhy, Removal of zinc ions from aqueous solution using a cation exchange resin, Chem. Eng. Res. Des. 91 (2013) 165–173.
[6] K. Bellir, M.B. Lehocine, A.-H. Meniai, Zinc removal from aqueous solutions by adsorption onto bentonite, Desalin. Water Treat. 51 (2013) 5035–5048.
[7] E. Marañón, Y. Fernández, F.J. Súarez, F.J. Alonso, H. Sastre, Treatment of acid pickling baths by means of anionic resins, Ind. Eng. Chem. Res. 39 (2000) 3370–3376.
[8] A. Çelekli, G. İlgün, H. Bozkurt, Sorption equilibrium, kinetic, thermodynamic, and desorption studies of

Reactive Red 120 on *Chara contraria*, Chem. Eng. J. 191 (2012) 228–235.
[9] D. Das, G. Basak, V. Lakshmi, N. Das, Kinetics and equilibrium studies on removal of zinc(II) by untreated and anionic surfactant treated dead biomass of yeast: Batch and column mode, Biochem. Eng. J. 64 (2012) 30–47.
[10] P.S. Koujalagi, S.V. Divekar, R.M. Kulkarni, R.K. Nagarale, Kinetics, thermodynamic, and adsorption studies on removal of chromium(VI) using Tulsion A-27(MP) resin, Desalin. Water Treat. 51 (2013) 3273–3283.
[11] S. Lagergren, About the theory of so-called adsorption of soluble substances, Kungliga Svenska Vetenskapsakademiens Handlingar 24(4) (1898) 1–39.
[12] Y.S. Ho, G. McKay, Pseudo-second order model for sorption processes, Process Biochem. 34 (1999) 451–465.
[13] Y.S. Ho, G. McKay, The kinetics of sorption of divalent metal ions onto sphagnum moss peat, Water Res. 34 (2000) 735–742.
[14] S.J. Elovich, Proceedings of the Second International Congress on Surface Activity, (Eds.) J. H. Schulman, Academic Press, Inc. New York, NY, 11 253–261 (1959).
[15] W.J. Weber Jr., R.R., Rumer, Intraparticle transport of sulfonated alkylbenzenes in a porous solid: Diffusion with nonlinear adsorption, Water Resour. Res. 1(3) (1965) 361–373.
[16] M.I. El-Khaiary, G.F. Malash, Y.-S. Ho, On the use of linearized pseudo-second-order kinetic equations for modeling adsorption systems, Desalination 257 (2010) 93–101.
[17] C. Namasivayam, D. Sangeetha, Removal and recovery of vanadium(V) by adsorption onto $ZnCl_2$ activated carbon: Kinetics and isotherms, Adsorption 12 (2006) 103–117.
[18] K.Y. Foo, B.H. Hameed, Insights into the modeling of adsorption isotherm systems, Chem. Eng. J. 156 (2010) 2–10.